

A Probody T Cell-Engaging Bispecific Antibody Targeting EGFR and CD3 Inhibits Colon Cancer Growth with Limited Toxicity



Leila M. Boustany, Sherry L. LaPorte, Laurie Wong, Clayton White, Veena Vinod, Joel Shen, Wendy Yu, David Koditek, Michael B. Winter, Stephen J. Moore, Li Mei, Linnea Diep, Yuanhui Huang, Shouchun Liu, Olga Vasiljeva, Jim West, Jennifer Richardson, Bryan Irving, Marcia Belvin, and W. Michael Kavanaugh

ABSTRACT

T cell-engaging bispecific antibodies (TCB) are highly potent therapeutics that can recruit and activate cytotoxic T cells to stimulate an antitumor immune response. However, the development of TCBs against solid tumors has been limited by significant on-target toxicity to normal tissues. Probody therapeutics have been developed as a novel class of recombinant, protease-activated antibody prodrugs that are “masked” to reduce antigen binding in healthy tissues but can become conditionally unmasked by proteases that are preferentially active in the tumor microenvironment (TME). Here, we describe the preclinical efficacy and safety of CI107, a Probody TCB targeting EGFR and CD3. *In vitro*, the protease-activated, unmasked CI107 effectively bound EGFR and CD3 expressed on the surface of cells and induced T-cell activation, cytokine release, and cytotoxicity toward tumor cells. In contrast, dually masked CI107 displayed a >500-fold reduction in antigen binding and >15,000-fold reduc-

tion in cytotoxic activity. *In vivo*, CI107 potently induced dose-dependent tumor regression of established colon cancer xenografts in mice engrafted with human peripheral blood mononuclear cells. Furthermore, the MTD of CI107 in cynomolgus monkeys was more than 60-fold higher than that of the unmasked TCB, and much lower levels of toxicity were observed in animals receiving CI107. Therefore, by localizing activity to the TME and thus limiting toxicity to normal tissues, this Probody TCB demonstrates the potential to expand clinical opportunities for TCBs as effective anticancer therapies for solid tumor indications.

Significance: A conditionally active EGFR-CD3 T cell-engaging Probody therapeutic expands the safety window of bispecific antibodies while maintaining efficacy in preclinical solid tumor settings.

Introduction

Bispecific antibodies that recruit cytotoxic T cells to tumors have demonstrated promise in recent years for the treatment of patients with cancer (1–4). These T cell-engaging bispecific (TCB) molecules are designed to bind two unique antigens, which can be achieved using a variety of molecular formats and configurations that can include single-chain variable fragments (scFv), full-length IgG, or F(ab') fragments, among others (5, 6). In the context of cancer therapy, these molecules can be targeted to bind to both a tumor-associated antigen and a cytotoxic T lymphocyte (CTL)-associated antigen, resulting in recruitment of the lymphocytes to the tumor and subsequent T cell-mediated cytotoxic effects. Although TCBs directed against numerous targets have been investigated, only one is currently approved for the treatment of cancer. Blinatumomab, an anti-CD3 x anti-CD19 TCB, has demonstrated efficacy in the treatment of patients with B-cell acute lymphoblastic leukemia, with the majority of patients achieving complete response after only one cycle of

treatment (2, 7). However, despite the clinical success of blinatumomab, the development of TCBs targeting antigens expressed in solid tumors has been limited by toxicities resulting from on-target, off-tumor activity in normal tissues and widespread immune activation (8–10). Recent efforts have focused on approaches to improve the specificity and selectivity of TCB molecules for tumors and T-cell subsets to mitigate these challenges (8, 11).

The development of Probody therapeutic candidates has enabled the potential improvement of tumor targeting of antibody therapeutics (12–16). Probody therapeutic antibodies are masked antibodies designed to be conditionally activated in the tumor microenvironment by tumor-associated proteases but not in normal tissues where protease activity is tightly controlled (17). A peptide mask blocking the antigen binding domain of the antibody is tethered to the antibody via a protease-cleavable linker. In normal tissues, this mask attenuates binding of the antibody therapeutic to the target protein. However, in the protease-rich tumor microenvironment, the linker is cleaved, releasing the peptide mask and enabling binding of the Probody therapeutic candidate to the target antigen. In nonclinical studies, Probody therapeutic candidates have demonstrated efficacy and improved safety compared with traditional antibodies in multiple antibody formats, including immunotherapies and Probody drug conjugates (12–15). A Probody drug conjugate targeting CD71, a previously “undruggable” target, has also demonstrated acceptable tolerability and preliminary clinical activity in a phase I trial in patients with solid tumors, highlighting the potential for Probody therapeutic candidates to improve the therapeutic windows for anticancer therapies in the clinical setting (16).

CytomX Therapeutics, Inc, South San Francisco, California.

Corresponding Author: Marcia Belvin, CytomX Therapeutics, Inc, South San Francisco, CA 94080. Phone: 650-892-9803, E-mail: mbelvin@cytomx.com

Cancer Res 2022;82:4288–98

doi: 10.1158/0008-5472.CAN-21-2483

This open access article is distributed under the Creative Commons Attribution-NonCommercial-NoDerivatives 4.0 International (CC BY-NC-ND 4.0) license.

©2022 The Authors; Published by the American Association for Cancer Research

Probody TCBs carry potential for improvements over traditional TCB approaches. Probody TCBs have been designed with protease-cleavable peptide masks that block both the tumor-associated antigen binding domain and the CD3 binding domain. In the tumor microenvironment, both peptide masks are removed, thus enabling improved tumor-selective activity of the TCB. Furthermore, the development of traditional TCBs is challenged by limited numbers of tumor-specific target antigens and narrow therapeutic windows, whereas Probody TCBs have the potential to both expand the landscape of available antigens for targeting solid tumors and reduce systemic toxicities due to the avoidance of T-cell engagement outside of the tumor microenvironment. Furthermore, traditional TCBs are also challenged with poor exposure due to target-mediated drug disposition (TMDD), whereas dramatically reduced TMDD is demonstrated with Probody TCBs because interaction with target outside of tumors is limited.

The EGFR is well known as a highly expressed oncogenic driver of tumor growth in multiple types of solid tumors. Four EGFR mAbs are currently approved for the treatment of cancer, but traditional antibody-based approaches to target EGFR have demonstrated limited lasting clinical responses due to activating mutations in downstream signaling proteins (18, 19). However, EGFR is an attractive candidate target for a Probody TCB because EGFR expression is prevalent across many tumor types. EGFR is also expressed in immunogenic indications, such as lung cancer and head and neck squamous cell carcinoma, providing the future possibility of combining treatment with other immunotherapeutic agents (20). In addition, the mechanism of action of a Probody TCB does not rely on blockade of EGFR signaling, and acquired resistance through mutational mechanisms may be less of a concern (21). Other TCB approaches for targeting EGFR have previously been described. T cell-engaging BiTE antibodies, designed on the basis of the binding domains of the approved EGFR antibodies cetuximab and panitumumab, have demonstrated potent antitumor effects (22, 23). However, acute toxicities associated with these molecules, including liver and kidney toxicity likely due to normal EGFR expression, led to discontinuation of their evaluation (22).

In this study, the nonclinical safety and efficacy of the Probody TCB CI107, an anti-EGFR x anti-CD3, were evaluated. As a Probody therapeutic, masking of both the EGFR and CD3 binding domains is intended to impair binding of CI107 to normal tissues, whereas protease activity within the tumor microenvironment results in unmasking, which allows binding to EGFR and CD3. Given the high levels of EGFR expression in multiple types of cancer, an anti-EGFR TCB has the potential to be an effective novel cancer therapeutic. Here, the therapeutic potential of a Probody TCB for the treatment of EGFR-expressing tumors is demonstrated by evaluating CI107 efficacy and safety in nonclinical models.

Materials and Methods

Animal studies

All animal studies were performed in accordance with and after approval from the appropriate Institutional Animal Care and Use Committee governing the facility that performed each study. Mouse xenograft studies were performed by CytomX Therapeutics, Inc (CytomX), and cynomolgus monkey studies were performed by Altasciences. All animal studies followed regulations set forth by the USDA Animal Welfare Act and the Guide for the Care and Use of Laboratory Animals.

Materials

All Probody TCBs and other antibodies described in this study, including CI107, CI128, CI020, CI011, CI040, CI048, and CI104, were generated by CytomX. Activated TCBs were generated by *in vitro* treatment with urokinase-type plasminogen activator followed by size exclusion chromatography (SEC) purification (13). HT29-Luc2 cells were obtained from Caliper Life Sciences, and HCT116, Lovo, Detroit-562, and Jurkat cells were obtained from ATCC. No additional authentication of cell lines or *Mycoplasma* testing was performed after purchase. Cells were cultured according to manufacturer's guidelines and working cell banks of no more than up to passage 5 were created. Working cell banks were stored in liquid nitrogen and, after thawing, were propagated for no more than 20 passages. Human peripheral blood mononuclear cells (PBMC) were obtained as cryopreserved vials of cells from individual donors from HemaCare Corporation, AllCells, or STEMCELL Technologies. NOD.Cg-Prkcd^{scid} Il2rg^{tm1Wjl/SzJ} (NSG) mice were obtained from Jackson Laboratories.

Cell binding assays

EGFR-expressing cells and Jurkat cells were maintained in complete media. EGFR-expressing cells were harvested using Versene cell dissociation buffer. Cells were centrifuged at 250 × g for 5–10 minutes and resuspended in FACS buffer containing 2% FBS (BD Pharmingen). Cells were plated at 150,000/well in V-bottom 96-well plates and treated with TCBs or *in vitro* protease-activated TCBs at various concentrations obtained by 3-fold serial dilutions in FACS buffer, starting at 1.5 μmol/L CI011, CI020, CI040, CI107, and CI128 for both EGFR-expressing and Jurkat cells, 0.05 μmol/L activated CI107 or CI048 for EGFR-expressing cells, and 0.5 μmol/L activated CI107 and CI048 for Jurkat cells. Cells were incubated for 1 hour at 4°C, washed twice with FACS buffer, and resuspended in 10 μg/mL Alexa Fluor 647 anti-human Fc secondary antibody. The cells were then incubated, protected from light, for 30–60 minutes at 4°C, washed twice with FACS buffer, resuspended in FACS buffer containing 7-aminoactinomycin D (7-AAD), and analyzed on a MACSQuant flow cytometer (Miltenyi Biotec). Mean fluorescence intensity data were corrected for secondary antibody background signal, graphed in Graphpad Prism, and EC₅₀ values were calculated.

Cytotoxicity assays

Luciferase-labeled target cells were plated into a 96-well white, flat-bottom, tissue culture-treated plate (Costar #3917) at 10,000 cells/well in RPMI + 5% human serum. Human PBMCs were freshly thawed and washed twice with RPMI + 5% human serum, and 100,000 PBMCs were added in RPMI + 5% human serum to the wells containing luciferase-labeled target cells. CI011, CI020, CI040, CI107, CI048, CI128, protease-activated CI107, or CI048 was then added to the wells at various concentrations obtained by 3-fold serial dilutions. Control wells contained untreated target + effector cells, target cells only, effector cells only, or media only. The plates were then incubated at 37°C and 5% CO₂ for approximately 48 hours. Cell viability was measured using the ONE-Glo Luciferase Assay System (Promega, #E6120) and a Tecan plate reader. The percent cytotoxicity was calculated as follows: (1-(RLU experimental/average RLU untreated))*100.

In vitro T-cell activation and cytokine analysis

T-cell activation was measured by induction of CD69 expression in PBMCs cocultured with HT29-Luc2 or HCT116-Luc2 cells. HT29-Luc2 or HCT116-Luc2 cells were plated at 10,000 cells/well in a U-bottom nonadherent plate. Human PBMCs were freshly thawed and

washed twice with RPMI containing serum, and 100,000 PBMCs/well were added to the plates containing tumor cells. Wells containing PBMCs only were seeded for flow cytometry compensation controls. Three-fold serial dilutions of CI107, activated CI107, or CI128 were prepared in media and added to the plated cells. Cells were incubated at 37°C and 5% CO₂ for 16 hours. To prepare for flow cytometry analysis, plates were centrifuged at 250 × g for 10–15 minutes. The supernatant was removed for cytokine analysis, Fc block (Human TruStain FcX, BioLegend) was added to each well, and the plates were incubated for 10 minutes. Antibody cocktails containing anti-CD45-FITC (BioLegend), anti-CD3-Pacific blue (BioLegend), anti-CD8a-APC (BioLegend), and anti-CD69-PE-Cy7 (BioLegend), or appropriate compensation controls were added to the wells, and the plates were incubated with shaking at 4°C protected from light for 30 to 60 minutes. The plates were then washed with FACS buffer and resuspended in FACS buffer containing 7-AAD. Fluorescence was measured using an Attune Flow Cytometer, and 15,000 events representing PBMCs were collected.

For cytokine analysis, Meso Scale Discovery U-PLEX plate assays (Meso Scale Diagnostics) were used. U-PLEX plates were prepared following the manufacturer's protocol to evaluate levels of MCP-1, TNFα, IL6, IL2, and IFNγ. Supernatant samples collected from HT29-Luc2 or HCT116-Luc2 cocultured with PBMCs and treated with CI107, activated CI107, or CI128 were diluted, added to the plate, and processed following the manufacturer's instructions.

In vivo efficacy studies

For *in vivo* experiments, effects of Probody TCBs on tumor growth were measured in mice harboring HT29-Luc2 or HCT116 tumors and engrafted with human T cells resulting from intraperitoneal injection of human PBMCs (24–26). Two million HT29-Luc2 or HCT116 cells were subcutaneously injected in 100 μL serum-free RPMI into the flank of female NSG mice on day 0. Frozen PBMCs from a single donor were freshly thawed and administered via intraperitoneal injection on day 3 in 100 μL RPMI + Glutamax, serum-free medium. PBMCs were previously characterized for CD3⁺ T-cell percentage, and the number of PBMCs to be used for *in vivo* administration was based on a CD3⁺ T cell to tumor cell (implanted) ratio of 1:1. Tumor measurements on approximately day 12 were used to randomize mice prior to intravenous dosing with TCB, control article, or vehicle. Animals were dosed weekly for 3 weeks with test articles, and tumor volumes and body weights were recorded twice weekly. Activated CI104 was used for

in vivo studies. CI104 differs from CI107 only in the cleavable linker used to tether the CD3 mask to the scFv (Table 1). Upon *in vitro* protease activation to fully remove the masks, activated CI104 is identical to activated CI107 and can be used to assess the activity of activated CI107, and subsequent *in vitro* cytotoxicity studies validated that the activity of activated CI104 is the same as that of activated CI107 (Supplementary Fig. S1). Both activated CI107 and activated CI104 are referred to as activated TCB.

Nonhuman primate safety studies

Male cynomolgus monkeys received slow intravenous bolus injection of test articles on day 1 or once on days 1 and 15, depending on the test article. Following test article administration, clinical observations were performed twice daily. Blood samples were collected at various timepoints postdose for analysis of cytokine release, serum chemistry, hematology, and toxicokinetics. Cytokine analysis was performed on serum samples using the Life Technologies Monkey Magnetic 29-Plex Panel Kit (Thermo Fisher Scientific). For toxicokinetic analysis, samples were processed to plasma and stored at –60°C to –86°C prior to shipment for analysis by AIT Bioscience or CytomX. Plasma concentrations of test articles were measured by ELISA using an anti-idiotypic capture antibody and an anti-human IgG (Fc) capture antibody. Toxicokinetic analysis was performed by Northwest PK Solutions using a noncompartmental analysis utilizing Phoenix WinNonlin v6.4 (Certara).

Data availability statement

All data relevant to the study are included in the article or Supplementary Data. The datasets used and/or analyzed in this study are available from the corresponding author upon reasonable request.

Results

Dual masking of anti-EGFR and anti-CD3 binding domains in the CI107 Probody TCB attenuates binding to cells expressing EGFR or CD3

The CI107 TCB was designed as a dual-masked tetravalent bispecific molecule containing anti-EGFR and anti-CD3 domains. CI107 was generated using a cetuximab-derived antibody with an SP34-derived anti-CD3ε scFv fused to the N terminus of the heavy chain. CI107 has a hIgG1 Fc with mutations that silence Fc function (Fig. 1; ref. 27). To generate CI107, a specific masking peptide for the anti-

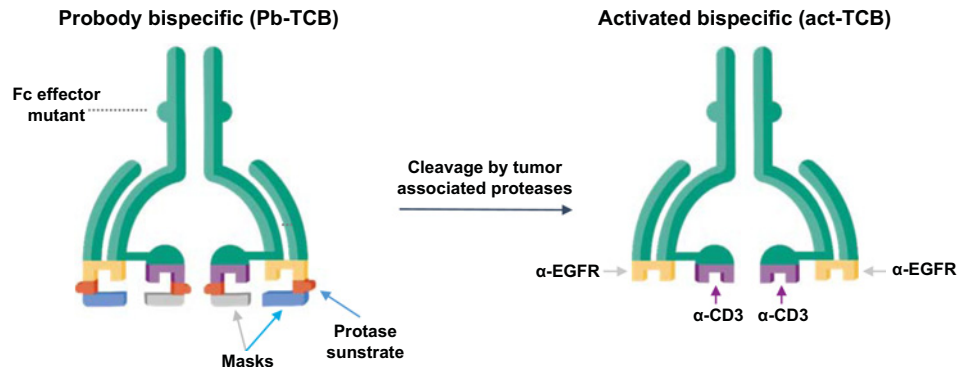
Table 1. Characteristics of Probody TCB molecules evaluated in these studies.

Molecule	EGFR mask	EGFR linker	EGFR linker cleavability	EGFR binder	CD3 mask	CD3 linker	CD3 linker cleavability	CD3 binder
CI011	Mask E1	Linker 1	+	C225v5	Mask C1	Linker 1	+	hSP34
CI020	Mask E1	Linker 5	Not cleavable	C225v5	Mask C1	Linker 5	Not cleavable	hSP34
CI040	Mask E1	Linker 2	++	C225v5	Mask C1	Linker 2	++	hSP34
CI048	N/A	N/A	N/A	C225v5	N/A	N/A	N/A	hSP34
CI104	Mask E1	Linker 3	+	C225v5	Mask C2	Linker 3	+	v16
CI107	Mask E1	Linker 3	+	C225v5	Mask C2	Linker 4	++	v16
CI128	No Mask	No Linker	N/A	Not targeted to EGFR	Mask C2	Linker 4	++	v16

Note: Probody TCB molecules used in these studies contain EGFR and CD3 binding domains, masks, and linker peptides with varying degrees of cleavability. CI011 and CI040 are first-generation versions of CI104 and CI107. The CI104 and CI107 molecules contain an optimized CD3 scFv, next-generation cleavable linkers, and additional Fc silencing mutations. CI104 and CI107 have the same masks and EGFR and CD3 binding domains, but differ in the CD3 protease linker; however, after protease activation, the activated TCB is the same. CI128 was used as a nontargeted control TCB in which the EGFR binder is replaced by an irrelevant antibody (anti-RSV). Abbreviation: N/A, not applicable.

Figure 1.

Design of Probody T cell-engaging bispecific therapeutic (Probody TCB). CI107 comprises a bispecific IgG antibody with EGFR and CD3 binding domains. Peptide masks of both binding domains are attached via a protease-cleavable linker. In normal tissues, these masks are designed to prevent binding to the target protein and to CD3⁺ lymphocytes. In contrast, cleavage of the linker by proteases present in the solid tumor microenvironment expose the EGFR and CD3 binding domains, enabling specific binding of the Probody TCB to the target antigen and CD3⁺ T cells.



EGFR antibody component was fused to the N terminus of the light chain using a protease-cleavable substrate linker flanked by flexible Gly-Ser-rich peptide linkers, as described previously (13). A masking peptide specific for the anti-CD3ε component was similarly added to the scFv using a protease-cleavable substrate linker. CI107 utilizes a full IgG bispecific format to maximize exposure and half-life and has impaired Fc-effector function to minimize cross-linking to cells expressing FcγR. The design of CI107 is intended to maximize target binding and activity in the protease-rich tumor microenvironment while minimizing binding and activity in normal tissues. Characteristics of Probody TCB molecules used throughout these studies, including molecule description, plasma stability, and the cleavability of CI107 (K_{cat}/K_M), are shown in Table 1, Supplementary Fig. S2, and Supplementary Table S1.

To assess whether masking of the EGFR binding domain impairs binding to EGFR expressed on the cell surface, binding of CI107 and activated TCB to EGFR-expressing HT29, HCT116, Lovo, and Detroit 562 cells was measured (Fig. 2; Supplementary Table S2; Supplementary Fig. S3).

Target cells were incubated with increasing concentrations of CI107 or activated TCB, and binding was evaluated by flow cytometry. The presence of the EGFR mask in CI107 substantially attenuated binding to EGFR expressed on the cell surface compared with activated TCB. Activated TCB bound to HT29 cells with a calculated K_d of 0.17 nmol/L, whereas the K_d for binding of CI107 was 91.28 nmol/L, representing a greater than 500-fold decrease in binding compared with activated TCB (Supplementary Table S2). Similar results were obtained using the other target cell lines. Binding of CI128, an

untargeted control TCB, which contains the same anti-CD3 module as CI107 but lacks EGFR targeting was also evaluated. This control TCB did not bind to the target cell lines tested (Fig. 2; Supplementary Table S2; Supplementary Fig. S3).

To determine whether masking of the anti-CD3 binding domain impairs binding of CI107 to CD3 on the surface of T lymphocytes, CI107 and activated TCB binding to Jurkat cells was measured. As shown in Fig. 2C and Supplementary Table S2, activated TCB bound to Jurkat cells with a K_d of 0.62 nmol/L. However, binding of CI107 was not detected, and a K_d could not be calculated. Activated control TCB CI128 bound Jurkat cells with similar affinity as activated TCB. Together, these data demonstrate reduced binding of the CI107 Probody TCB to cellularly expressed EGFR and CD3 compared with the activated TCB.

Masking significantly attenuates cytotoxicity and T-cell activation in PBMCs coculture with human cancer cells

To address whether targeting EGFR with the Probody TCB CI107 could lead to antitumor cell effects, *in vitro* cytotoxicity assays were performed. Previous studies have demonstrated that cetuximab is not directly cytotoxic to HT29 or HCT116 cells (28). Here, luciferase-expressing target cells with a range of EGFR expression levels (Supplementary Fig. S3C) were cocultured with human PBMCs and incubated with increasing concentrations of CI107, protease-activated TCB, or the untargeted control TCB CI128. After 48 hours of culture, viability of the target cells was measured via luciferase assay. As shown in Fig. 3A, treatment with the control CI128 resulted in minimal cytotoxicity to HCT116-Luc2 cells cocultured with PBMCs,

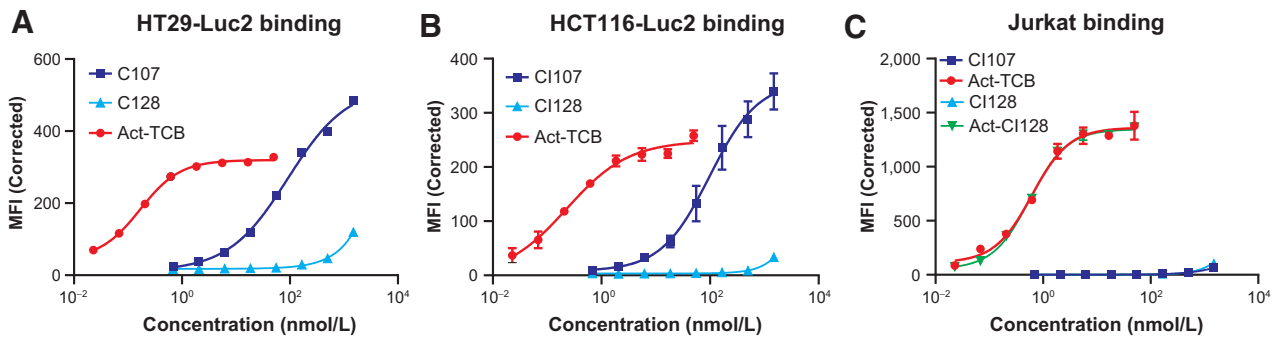


Figure 2.

Dual masking of the anti-EGFR and anti-CD3 binding domains attenuates binding of CI107 to EGFR and CD3 expressed on the surface of cells. HT29 (A), HCT116 (B), or Jurkat (C) cells were incubated with increasing concentrations of CI107 or protease-activated TCB (Act-TCB), and binding was assessed by flow cytometry.

demonstrating that engagement of both EGFR and CD3 is required for cytotoxic activity. In contrast, both CI107 and activated TCB had cytotoxic effects on HCT116-Luc2 cells. However, activated TCB resulted in cytotoxicity at much lower concentrations compared with the masked form, with EC_{50} values of 0.44 pmol/L and 7,297 pmol/L, respectively. Similar results were observed in HT29-Luc2 cells (Fig. 3B), with EC_{50} values of 0.25 pmol/L for activated TCB versus 3,678 pmol/L for CI107 as well as for additional target cell lines and PBMC donors (Supplementary Table S3). Therefore, for HCT116 and HT29 cells, dual masking of the anti-EGFR and anti-CD3 domains in CI107 resulted in an approximately 15,000-fold decrease in cytotoxic activity mediated by PBMCs in the absence of protease activation of this Probody therapeutic. The magnitude of this decrease varied across cell lines and donors.

To determine whether CI107 results in T-cell activation, CD69 levels in PBMCs cocultured with HCT116-Luc2 or HT29-Luc2 cells were measured after treatment with CI107, activated TCB, and control CI128. CD69 acts as a marker of T-cell activation; after TCR/CD3 engagement, CD69 expression is rapidly induced on the surface of T lymphocytes and acts as costimulatory molecule for T-cell activation and proliferation (29, 30). Human PBMCs cocultured with HCT116-Luc2 or HT29-Luc2 cells were treated with increasing concentrations of CI107, activated TCB, or control CI128 for 16 hours, and CD69 expression levels were measured by flow cytometry. As shown in Fig. 3C and Supplementary Table S4,

CI107 resulted in induction of CD69 expression on $CD8^+$ T cells cocultured with HCT116-Luc2 cells with an EC_{50} of 14178 pmol/L. In contrast, treatment with activated TCB resulted in CD69 induction with an EC_{50} of 7.65 pmol/L, reflecting an approximately 1,800-fold shift in the T-cell activation curve compared with CI107. Importantly, T-cell activation was not observed with the non-EGFR targeted control TCB CI128, indicating that engagement of CD3 alone is not sufficient for T-cell activation. Similarly, treatment of PBMCs from the same donor cocultured with HT29-Luc2 cells resulted in CD69 induction with EC_{50} values of 65971 pmol/L for masked CI107 versus 8.75 pmol/L for activated TCB, reflecting an approximately 7,500-fold difference in CD69 induction capacity (Fig. 3D; Supplementary Table S4). Similar results were seen using PBMCs from additional donors (Supplementary Table S4).

To further assess T-cell activation in PBMCs cocultured with EGFR-expressing cancer cells upon treatment with Probody TCB, cytokine release was evaluated after treatment with CI107, activated TCB, or control CI128. Levels of $IFN\gamma$, IL2, IL6, MCP-1, and $TNF\alpha$ were measured 16 hours after treatment with increasing concentrations of Probody TCB. As shown in Fig. 4, treatment with CI107 at concentrations in the 10^4 pmol/L range resulted in release of each of the cytokines measured. In contrast, activated TCB resulted in cytokine release upon treatment with concentrations in the 1–100 pmol/L range. These results were generally consistent between different PBMC donor cells and cancer cell lines (HCT116-Luc2 vs. HT29-Luc2;

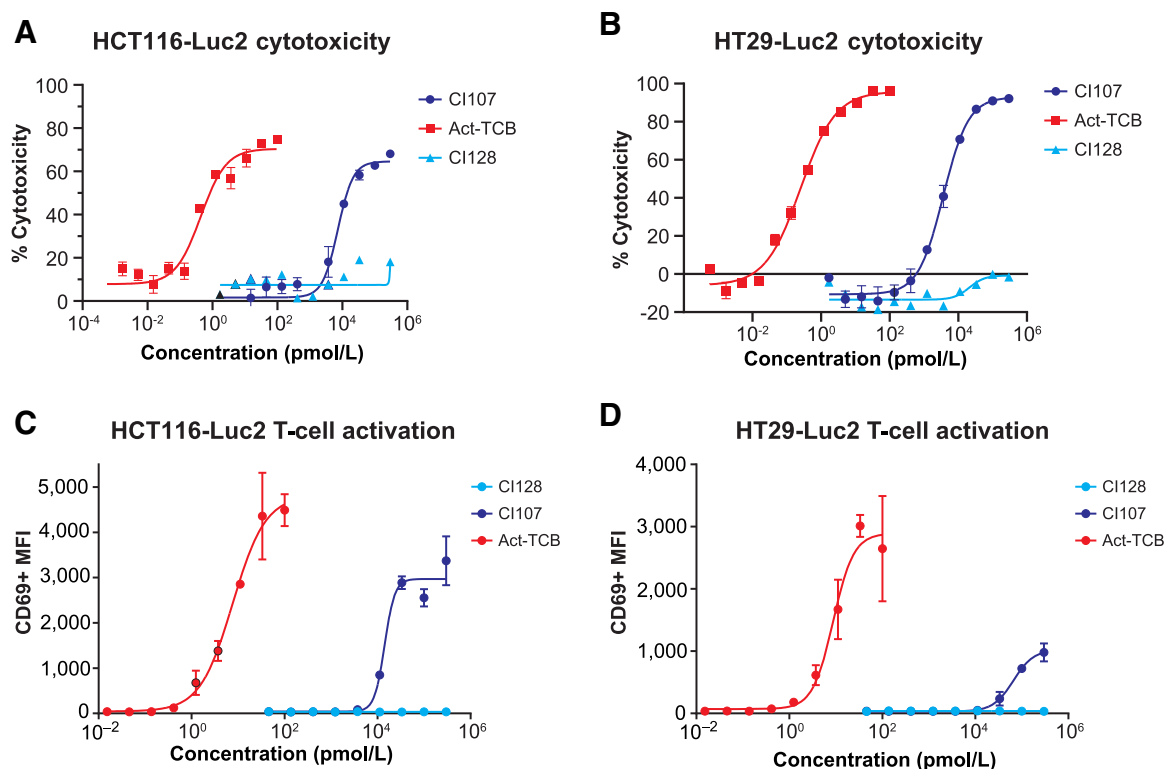


Figure 3.

Masking of EGFR and CD3 binding domains attenuates cytotoxicity and T-cell activation mediated by CI107 in PBMCs cocultured with human colorectal cancer cells. HCT116-Luc2 (A and C) and HT29-Luc2 (B and D) cells were cocultured with human PBMCs (Donor 4) and treated with increasing concentrations of CI107, activated TCB (Act-TCB), or non-EGFR-targeted control CI128. A and B, After 48 hours of culture, HCT116-Luc2 or HT29-Luc2 cell viability was measured by the ONE-Glo Luciferase Assay, and cytotoxicity was measured relative to untreated controls. C and D, After 16 hours of culture, CD69 expression in PBMCs was measured by flow cytometry. MFI, mean fluorescence intensity.

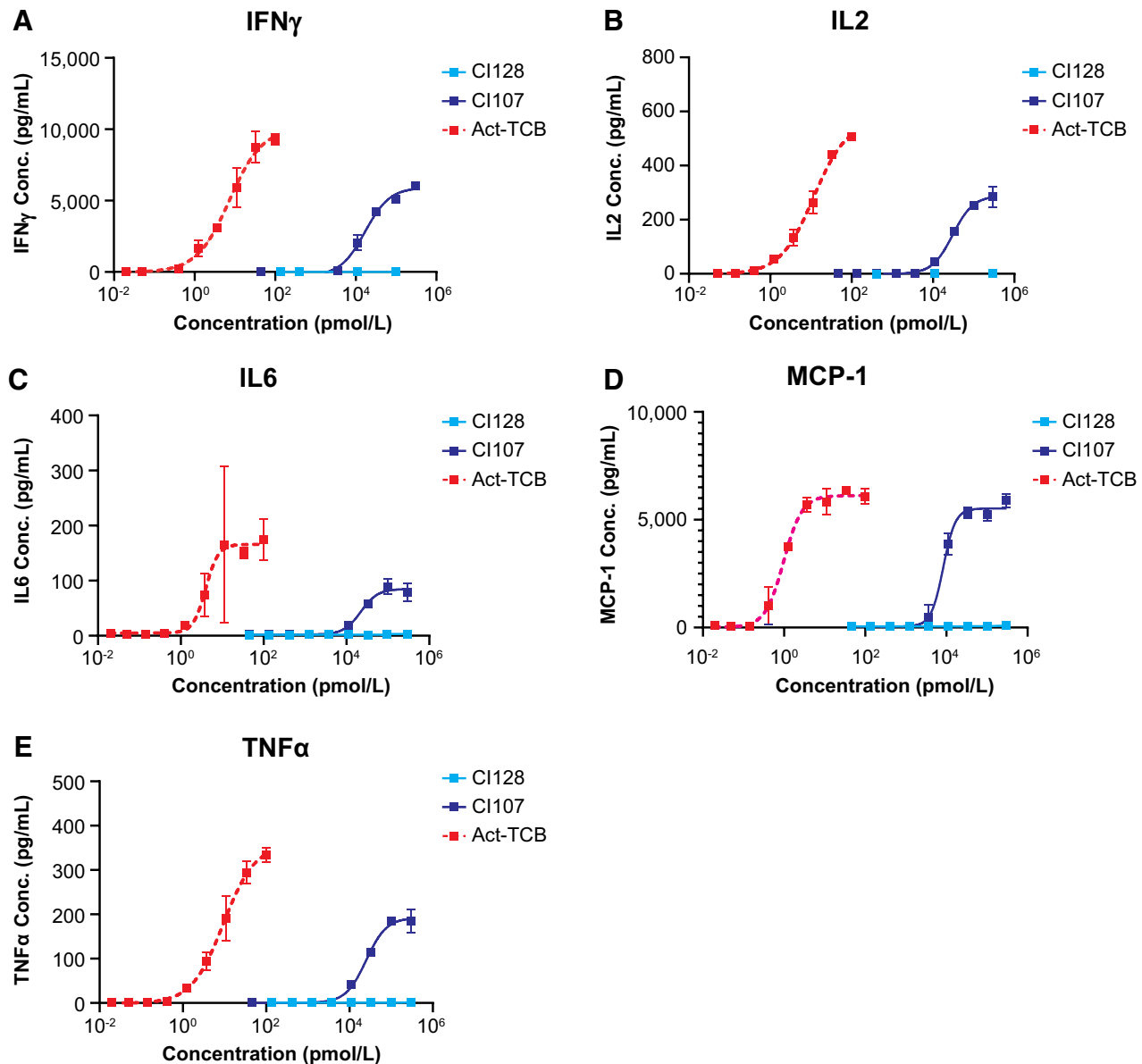


Figure 4.

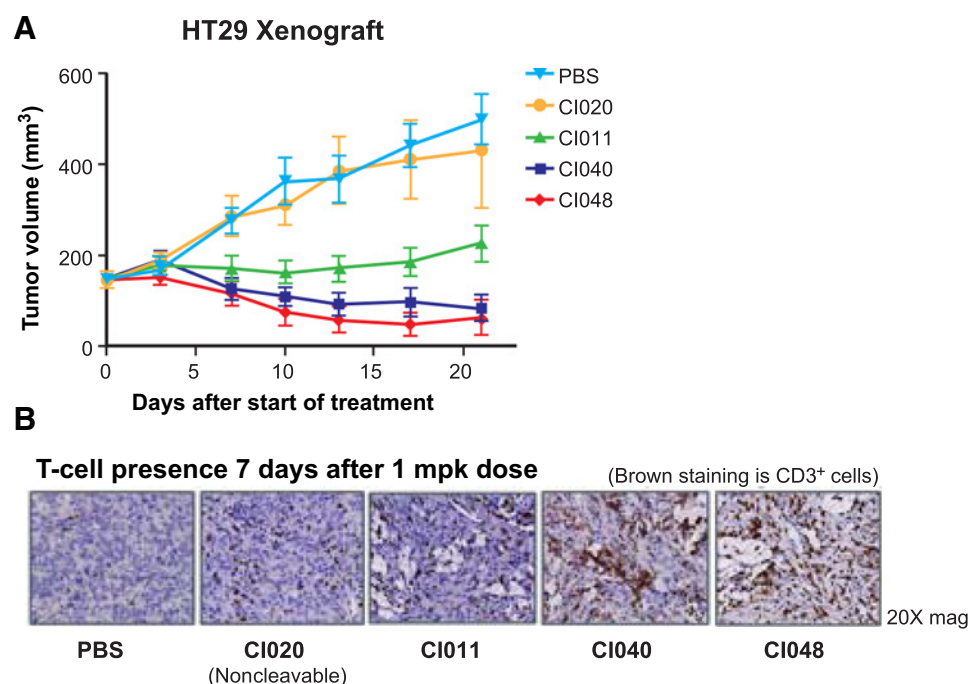
Masking of EGFR and CD3 binding domains in CI107 attenuates cytokine release in PBMCs cocultured with human colorectal cancer cells. HCT116-Luc2 cells were cocultured with human PBMCs (Donor 4) and treated with increasing concentrations of CI107, activated TCB (Act-TCB), or non-EGFR-targeted control CI128. After 16 hours of culture, cytokine release was measured for IFN γ (A), IL2 (B), IL6 (C), MCP-1 (D), and TNF α (E) using a U-PLEX plate.

Supplementary Table S5). Together, these data demonstrate that dual masking of the EGFR and CD3 binding domains in CI107 attenuates T-cell activation in the absence of protease activation.

Probody TCB sensitivity to protease cleavage correlates with *in vivo* antitumor efficacy and intratumoral T cells

Given the cytotoxic activity of CI107 *in vitro*, antitumor efficacy of Probody anti-EGFR x anti-CD3 TCBs was evaluated *in vivo*. Immunocompromised mice harboring HT29-Luc2 tumors and engrafted with human PBMCs were treated once weekly for 3 weeks with vehicle (PBS) or 0.3 mg/kg of Probody TCBs containing linkers with different protease sensitivities (CI111, CI040), a noncleavable

linker (CI020), or the unmasked bispecific therapeutic CI048, as described in Table 1. CI020 is expected to have minimal antitumor activity due to the noncleavable linker, whereas unmasked CI048 is expected to have maximal efficacy. CI011 and CI040, which both contain EGFR and CD3 masks, have differing protease sensitivities due to different linker peptides in the prodomains; CI040 is cleavable by a broader set of proteases than CI011. Similar to CI107, binding of CI011, CI020, and CI040 to EGFR and CD3 is attenuated (Supplementary Fig. S4); however, the magnitude of CD3 binding attenuation is reduced for these Probody TCBs due to a weaker CD3 mask. Similarly, the cytotoxic activity of these molecules is less attenuated than CI107 when compared with the

**Figure 5.**

Sensitivity of Probody TCB to protease cleavage correlates with efficacy and intratumoral T-cell presence in PBMC-engrafted NSG mice. **A**, NSG mice harboring HT29-Luc2 tumors and engrafted with human PBMCs were treated on days 1, 8, and 15 with vehicle (PBS) or 0.3 mg/kg CI020, CI011, CI040, or CI048 ($n = 8$ per group). Tumor volume was measured twice weekly. **B**, NSG mice harboring HT29-Luc2 tumors and engrafted with human PBMCs were treated with vehicle or 1 mg/kg of CI020, CI011, CI040, or CI048. Tumors were harvested 7 days after dosing, and immunohistochemistry for CD3 was performed. Brown stain indicates CD3⁺ cells.

unmasked TCB, which is consistent with the weaker masking of these molecules (Supplementary Fig. S5).

As shown in Fig. 5A, treatment with the unmasked TCB CI048 led to tumor regressions within 1 week after the start of treatment. Similarly, the masked Probody TCBs CI011 and CI040 also resulted in tumor regression or stasis; the regression seen with CI040 correlates with the greater cleavability of the linkers in this molecule compared with CI011. In contrast, treatment with CI020, which contains non-cleavable linkers, did not affect tumor growth, indicating that protease cleavability is required for antitumor activity of the Probody TCB *in vivo*.

To determine whether the antitumor efficacy mediated by the Probody TCBs tested correlates with T-cell presence in the tumors, tumors were harvested 1 week after animals received a 1 mg/kg dose of Probody TCB or activated TCB, and IHC for CD3 was performed. As shown in Fig. 5B, minimal numbers of T cells were observed in tumor tissue after treatment with vehicle or the noncleavable CI020. In contrast, increased numbers of T cells were observed upon treatment with the Probody TCB CI040 or the *in vitro* protease-activated TCB CI048. Again, the Probody TCB with greater protease sensitivity (CI040) resulted in greater numbers of T cells in the tumor. Together, these data suggest that Probody TCBs can result in intratumoral T cells and antitumor efficacy *in vivo* that correlates with sensitivity to protease cleavage of the EGFR and CD3 binding domain masks.

CI107 induces dose-dependent regressions of established xenograft tumors in PBMC-engrafted NSG mice

Given the proof of concept provided by the *in vivo* efficacy studies of the first-generation Probody TCBs CI011 and CI040 from which CI107 was developed, the effects of CI107 on *in vivo* tumor growth were evaluated. NSG mice were subcutaneously implanted with HT29 cells followed by intraperitoneal injection of PBMCs, and PBMCs were allowed to engraft for approximately 11 days. Animals were then treated with vehicle, 0.5 mg/kg CI107, or 1.5 mg/kg CI107 once weekly for 3 weeks. As shown in Fig. 6A, treatment with 0.5 mg/kg CI107

resulted in tumor stasis and 1.5 mg/kg CI107 led to tumor regression starting approximately 1 week after treatment initiation.

The *in vivo* efficacy of CI107 was also evaluated in HCT116 tumors. After tumor and PBMC engraftment, animals were treated with vehicle, 0.3 mg/kg CI107, 1 mg/kg CI107, or 0.3 mg/kg activated TCB. As shown in Fig. 6B, 0.3 mg/kg CI107 delayed HCT116 tumor growth, whereas 1 mg/kg CI107 and 0.3 mg/kg activated TCB resulted in similar levels of tumor regression and stasis for the duration of treatment. Together, these data demonstrate that CI107 induces dose-dependent inhibition of tumor growth and regression in HT29 and HCT116 xenograft tumors and that the antitumor activity of a 3-fold higher dose of CI107 is similar to that of activated TCB.

CI107 provides increased safety relative to activated TCB in cynomolgus monkeys

The nonclinical tolerability of CI107 was evaluated in cynomolgus monkey studies. Animals received a single administration of 0.06 or 0.18 mg/kg activated TCB and 0.6, 2.0, 4.0, or 6.0 mg/kg CI107, and animals were followed for clinical observations. Animals treated with 0.18 mg/kg activated TCB experienced severe clinical effects, including emesis, inappetence, pale appearance, hunched posture, and thin appearance, with adverse effects noted as early as 2 hours and up to 10 days postdose (Supplementary Table S6). Animals treated with 0.06 mg/kg activated TCB experienced moderate and transient clinical effects, including emesis and hunched posture on day 1 postdose; based on the rapid resolution of these effects, 0.06 mg/kg was defined as the MTD for activated TCB. In contrast, animals treated with 2.0 mg/kg CI107 experienced only transient and mild clinical effects (emesis on day 1 or 2), and animals treated with 0.6 mg/kg CI107 did not experience any adverse effects. Animals treated with 4.0 mg/kg CI107 experienced moderate clinical effects (including emesis at 4, 8, and 24 hours after dose and inappetence on day 2). The animal treated with 6.0 mg/kg CI107 was found dead on day 2. Clinical signs noted prior to death included hunched posture, pale appearance, emesis, and liquid feces after dose. Therefore, 4.0 mg/kg was considered the MTD for

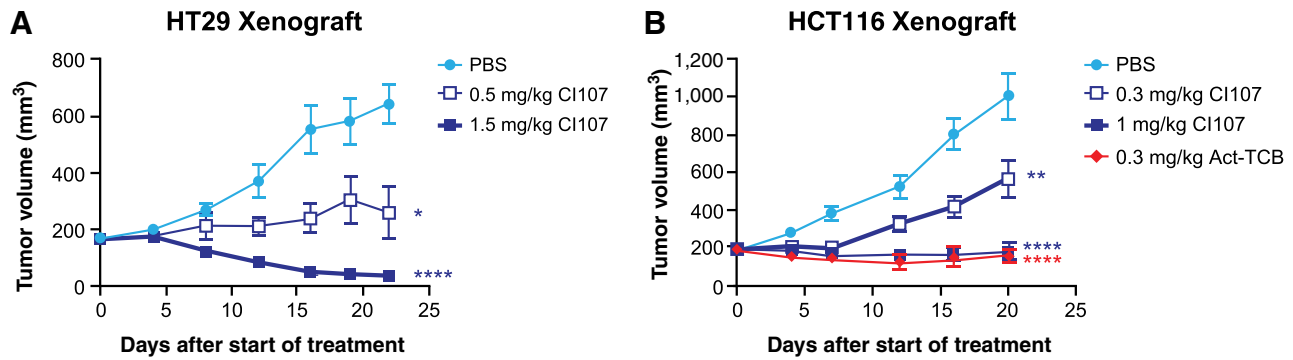


Figure 6. CI107 induces dose-dependent regression of xenograft tumors in PBMC-engrafted NSG mice. NSG mice harboring HT29 (A) or HCT116 (B) xenograft tumors and engrafted with human PBMCs were treated with CI107 once weekly for 3 weeks. Tumor volume was measured twice weekly. *, $P < 0.5$; **, $P < 0.01$; ****, $P < 0.0001$.

CI107. Overall, CI107 achieved a greater than 60-fold improvement in tolerability compared with activated TCB.

Cytokine levels were also examined after treatment with activated TCB or CI107. As shown in Fig. 7A, levels of IL6 and IFN γ were elevated in animals treated with activated TCB at 8 hours after dosing. In contrast, minimal changes in IL6 or IFN γ were observed after treatment with 0.6 or 2.0 mg/kg CI107; elevated levels of these cytokines were seen only after treatment with 4.0 mg/kg CI107 and are correlated with the acute adverse events observed. Consistent with the clinical observations, CI107 shifts the cytokine release dose response by more than 60-fold.

Analysis of serum chemistry also demonstrated differences between activated TCB and CI107. As shown in Fig. 7B, treatment with activated TCB led to dose-dependent increases in aspartate aminotransferase (AST), a marker of hepatocellular injury, at 48 hours postdose. In contrast, no changes in AST were observed after treatment with CI107 at any of the tolerated dose levels, demonstrating improved tolerability with this Probody TCB.

To address whether masking of the EGFR and CD3 binding domains affects the pharmacokinetics of the TCB, the plasma concentrations of activated TCB and CI107 after dosing were measured. As shown in Fig. 7C, activated TCB was rapidly cleared from

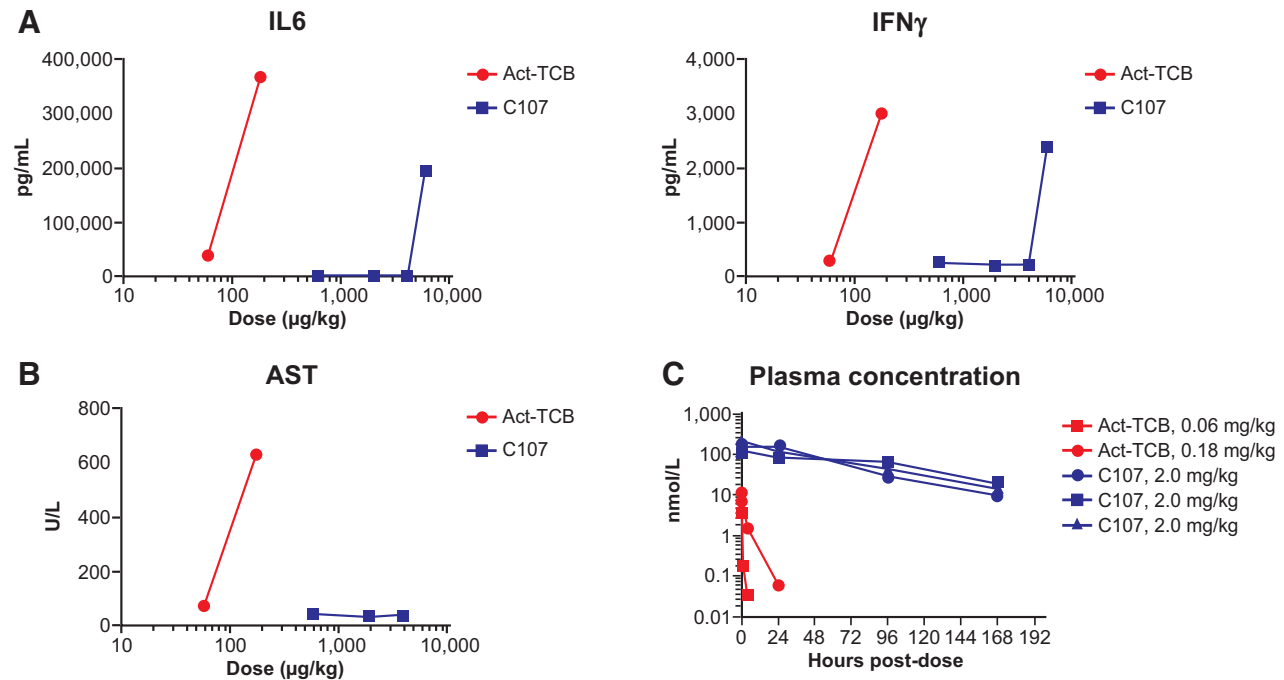


Figure 7. CI107 provides improved tolerability and exposure relative to Act-TCB in cynomolgus monkeys. Cynomolgus monkeys were administered a single dose of 0.06 or 0.18 mg/kg of activated TCB (Act-TCB) on day 1 or 0.6, 2.0, 4.0, or 6.0 mg/kg CI107. **A**, Levels of IL6 and IFN γ were measured 8 hours after dosing. Cytokine analysis was performed with a Luminex suspension array system on serum samples. **B**, Levels of AST were measured by serum chemistry analysis 48 hours after dosing. **C**, Plasma concentrations of Act-TCB and CI107 were measured by ELISA using anti-idiotype capture and anti-human Fc detection. Blue lines in **C** represent data from three individual animals dosed with 2.0 mg/kg CI107; red lines represent single animals dosed with 0.06 or 0.18 mg/kg Act-TCB.

circulation within 24 hours after dosing. In contrast, CI107 was maintained in the plasma for up to 7 days after dosing, suggesting that masking may increase exposure relative to the activated TCB. $AUC_{(0-7)}$ following single administration of activated TCB at 0.06 mg/kg was 0.04 day*nmol/L ($n = 1$), while $AUC_{(0-7)}$ following administration of CI107 at 2 mg/kg was 331.7 day*nmol/L (average of $n = 3$), demonstrating a greater than 8,000-fold increase in tolerated exposure. Together, the improvements in tolerability and pharmacokinetics observed with CI107 are consistent with the expected attenuation of binding to EGFR and CD3 in the normal tissue environment.

Discussion

Bispecific antibody therapeutic candidates targeting a variety of tumor antigens have demonstrated potent efficacy in nonclinical models, but the tolerability and safety challenges associated with these molecules have limited their clinical development. The studies presented here evaluated an anti-EGFR x anti-CD3 Probody TCB. These studies aimed to determine whether conditional masking of the antigen binding domains could minimize CI107 binding and activity in normal tissues in the absence of tumor-associated proteases while maintaining efficacy in the tumor microenvironment. Our data demonstrate that compared with the activated TCB, masking of the EGFR and CD3 binding domains substantially reduces binding to cells expressing EGFR or CD3 and attenuates CI107-mediated cytotoxicity and T-cell activation in PBMCs cocultured with EGFR-expressing cells in conditions with minimal protease activity. Furthermore, CI107 displays potent efficacy against xenograft tumors in mice engrafted with human PBMCs and improved tolerability and exposure compared with activated TCB in cynomolgus monkeys.

As one of the most commonly expressed or overexpressed solid tumor surface antigens, EGFR represents a strong candidate target for a Probody TCB. Previous efforts to develop TCBs targeting EGFR have demonstrated potent efficacy, but target-mediated toxicity to normal tissues has limited their development (22, 31). A Probody therapeutic candidate is designed to impair binding and activity of the anti-EGFR x anti-CD3 TCB in the normal tissue environment. Our data demonstrate that dual masking of the EGFR and CD3 binding domains in CI107 effectively attenuates binding of the Probody TCB to cells expressing EGFR or CD3 in the absence of protease activation. Notably, Probody therapeutics are not inert molecules as the interaction between the mask and antibody is dynamic and the mask has both bound and unbound states. Therefore, at high concentrations of intact Probody therapeutic, some target binding and functional activity is expected. In contrast, protease-activated TCB has apparent affinity for cell surface-expressed EGFR and CD3 in the low nanomolar range. Consistent with the binding data, activated TCB can induce CD69 expression, cytokine release, and cytotoxicity to tumor cells from human PBMCs cocultured with colorectal cancer cells, demonstrating the efficacy of this molecule in stimulating a T-cell response to target the tumor cells. In contrast, the fully masked form of CI107 displayed an approximately 15,000-fold reduced capacity to induce cytotoxicity, demonstrating the ability of masking to greatly attenuate functional activity in conditions with low protease activity.

However, the Probody TCB still retains potent anti-tumor activity *in vivo* where protease activity in the tumor microenvironment is high. We expect CI107 will reach the tumor through normal mechanisms of macromolecule biodistribution. Once in the tumor, protease activation

of CI107 allows target binding and retention of the molecule in the TME. In general, biodistribution of Probody therapeutics is similar to their parental antibodies (14, 15). Notably, a mouse cross-reactive Probody therapeutic targeting PD-L1 showed similar tumor uptake to the parent antibody and only modest uptake in lymphoid organs and other normal tissues expressing PD-L1 (15). Furthermore, successful targeting of masked Probody therapeutic to tumor lesions has been demonstrated in patients using ^{89}Zr -labeled PD-L1 Probody therapeutics (32).

Probody TCB efficacy and presence of CD3⁺ T cells in the tumor correlated with the cleavability of the linker substrate. Treatment with activated TCB resulted in rapid and dramatic HT29 tumor regressions and corresponded with high numbers of CD3⁺ T cells in the tumor. Similarly, treatment with Probody TCBs containing linkers with differing protease sensitivities also led to increased T cells in the tumors and antitumor activity. These responses correlated with the cleavability of the masked Probody TCB molecule, with the masked Probody TCB molecule containing the more cleavable linker demonstrating increased presence of intratumoral T cells and tumor regression compared with tumor stasis for the Probody TCB with the less cleavable linker. In contrast, a Probody TCB containing a noncleavable substrate demonstrated minimal intratumoral T cells and no effects on tumor growth, suggesting that antitumor efficacy is dependent on protease cleavage of the linker and release of the EGFR and CD3 binding domain masks that occurs in the solid tumor microenvironment. Notably, many patient tumors exhibit immunosuppressive tumor microenvironments with poor T-cell infiltration (33, 34), which are expected to hinder activity of this modality. To increase the potential for clinical benefit, indications with high EGFR expression and inflamed tumor microenvironments such as non-small cell lung cancer could be selected. Treatment of animals with HT29 and HCT116 xenograft tumors with CI107 further confirmed the dose-dependent antitumor efficacy of the Probody TCB in the *in vivo* tumor setting. Because HT29 and HCT116 are *BRAF*- and *KRAS*-mutant cell lines, respectively, and not responsive to cetuximab, the antitumor efficacy of CI107 demonstrates the potential therapeutic advantages of the Probody TCB for targeting EGFR-expressing tumors (22, 35). We have not evaluated combination treatment in our models; however, the potential for improved efficacy of TCBs in combination with checkpoint inhibitors or costimulatory molecules has been demonstrated preclinically (36, 37) and is currently under clinical investigation (38–44). Although the translational relevance of mouse xenograft models is limited, the potent nonclinical efficacy data combined with improved safety of the Probody TCB support advancing an EGFR-CD3 Probody TCB to clinical investigation.

Evaluation of safety in mouse models would be a valuable approach to define the efficacy and/or safety balance of Probody TCBs; however, this requires mouse models in which both the target and CD3 are humanized because of the lack of rodent cross reactivity of CI107. Therefore, tolerability of CI107 was evaluated in cynomolgus monkeys. Compared with protease-activated TCB, CI107 demonstrated a 60-fold increase in the MTD and no clinical signs were observed in animals dosed with a 10-fold higher dose of CI107 than the MTD for the activated TCB. All clinical signs observed at higher doses of CI107 up to 4 mg/kg were transient and resolved within 2 days of dosing. EGFR-targeted therapies, such as cetuximab, are known to have dermatologic effects including rash (45). However, we did not observe any skin rash in cynomolgus monkeys treated with CI107 nor was it observed with an EGFR Probody therapeutic dosed at 24 mg/kg for 4 weeks following a loading dose of 40 mg/kg (13). CI107 also

demonstrated reduced cytokine release and no increase in AST levels, whereas increased IL6, IFN γ , and AST levels were observed after administration of the activated TCB. These differences suggest that dual masking of the EGFR and CD3 binding domains in CI107 dramatically improve the tolerability and safety of the Probody TCB. Although a 3-fold higher dose of the Probody TCB is needed to induce the same antitumor activity in mouse efficacy models as the activated TCB, there is a 60-fold increase in MTD of the Probody TCB in cynomolgus monkey supporting an increased safety window.

The plasma concentration of CI107 compared with the activated TCB after dosing in cynomolgus monkeys further highlights the improved potential of a Probody TCB therapeutic. CI107 was maintained in the serum for up to 1 week after dosing, in contrast with the activated TCB, which was cleared within 24–48 hours of administration. Unmasked molecule in circulation could increase the potential for toxicity due to target engagement in normal tissues, and others have addressed this concern by engineering bispecific formats with a short half-life active species (46). However, our clinical data for a PD-L1 Probody therapeutic (pacmilimab) shows that it is largely intact in circulation (47). In addition, preclinical data for a CD137-targeted Probody therapeutic demonstrated that minimal activated molecule reached tumor draining lymph nodes (48). Therefore, although unmasked molecule could pose a safety concern, our data indicate that Probody therapeutics remain masked in circulation and recirculation of cleaved molecule is minimal.

Together, these nonclinical studies displaying potent anti-tumor activity combined with improved safety demonstrate the potential advantages of a Probody TCB therapeutic and provide a foundation for clinical evaluation of the EGFR-CD3 target combination. Notably, the clinical potential of Probody therapeutics has been demonstrated for several molecules across targets and modalities including the anti-PD-L1 Probody therapeutic pacmilimab (49), anti-CD166 Probody drug conjugate praluzatamab ravtansine (50), and the anti-CD71 Probody drug conjugate CX-2029 (16). The challenges of targeting solid tumors with T-cell bispecifics are well known and include toxicities resulting from target expression on normal tissue and systemic cytokine release (51, 52). Leveraging the Probody platform may help to mitigate these toxicities; however, common strategies employed in clinical studies to address T-cell bispecific platform toxicities including step dosing, treatment with corticosteroids, and careful monitoring of cytokine release should also be considered when evaluating a Probody TCB in the clinic. The nonclinical studies presented here demonstrate

the potential of the Probody T-cell bispecific approach for targeting solid tumors and support the development of this modality for the treatment of cancer.

PROBODY is a U.S. registered trademark of CytomX Therapeutics, Inc.

Authors' Disclosures

L.M. Boustany reports a patent for US2019/133747 pending. S.L. LaPorte reports other support from CytomX during the conduct of the study; other support from CytomX outside the submitted work; in addition, S.L. LaPorte has a patent for US10,669,337 issued and a patent for US2019/133747 pending. C. White reports a patent for US patent US10,669,337 issued. S. Moore is a former employee of and shareholder in Cytomx. B. Irving reports a patent for US10,669,337 issued and a patent for US2019/133747 pending. W.M. Kavanaugh reports other support from Amgen during the conduct of the study; personal fees from CytomX Therapeutics, Inc., outside the submitted work; in addition, W.M. Kavanaugh has a patent for Multiple pending and issued; and W.M. Kavanaugh is and/or has been a stockholder, employee, and paid consultant and advisor to CytomX Therapeutics, Inc. No disclosures were reported by the other authors.

Authors' Contributions

L.M. Boustany: Conceptualization. **S.L. LaPorte:** Conceptualization. **L. Wong:** Conceptualization. **C. White:** Conceptualization. **V. Vinod:** Conceptualization. **J. Shen:** Conceptualization. **W. Yu:** Conceptualization. **D. Koditek:** Conceptualization. **M.B. Winter:** Conceptualization. **S.J. Moore:** Conceptualization. **L. Mei:** Conceptualization. **L. Diep:** Conceptualization. **Y. Huang:** Conceptualization. **S. Liu:** Conceptualization. **O. Vasiljeva:** Conceptualization. **J. West:** Conceptualization. **J. Richardson:** Conceptualization. **B. Irving:** Conceptualization. **M. Belvin:** Conceptualization. **W.M. Kavanaugh:** Conceptualization.

Acknowledgments

This study was funded by CytomX Therapeutics, Inc., South San Francisco, CA. The authors thank Dylan Daniel for critical review of the article. Medical writing support was provided by Shirley Markant, PhD, through Phillips Gilmore Oncology Communications, Inc.

The publication costs of this article were defrayed in part by the payment of publication fees. Therefore, and solely to indicate this fact, this article is hereby marked "advertisement" in accordance with 18 USC section 1734.

Note

Supplementary data for this article are available at Cancer Research Online (<http://cancerres.aacrjournals.org/>).

Received October 26, 2021; revised May 9, 2022; accepted September 14, 2022; published first September 16, 2022.

References

- Kantarjian H, Stein A, Gokbuget N, Fielding AK, Schuh AC, et al. Blinatumomab versus chemotherapy for advanced acute lymphoblastic leukemia. *N Engl J Med* 2017;376:836–47.
- Gökbuget N, Dombret H, Bonifacio M, Reichle A, Graux C, Faul C, et al. Blinatumomab for minimal residual disease in adults with B-cell precursor acute lymphoblastic leukemia. *Blood* 2018;131:1522–31.
- Guy DG, Uy GL. Bispecific antibodies for the treatment of acute myeloid leukemia. *Curr Hematol Malig Rep* 2018;13:417–25.
- Caraccio C, Krishna S, Phillips DJ, Schürch CM. Bispecific antibodies for multiple myeloma: a review of targets, drugs, clinical trials, and future directions. *Front Immunol* 2020;11:501.
- Trabolsi A, Arumov A, Schatz JH. T cell-activating bispecific antibodies in cancer therapy. *J Immunol* 2019;203:585–92.
- Wu Z, Cheung NV. T cell engaging bispecific antibody (T-BsAb): from technology to therapeutics. *Pharmacol Ther* 2018;182:161–75.
- Locatelli F, Zugmaier G, Rizzari C, Morris JD, Gruhn B, Klingebiel T, et al. Effect of blinatumomab vs chemotherapy on event-free survival among children with high-risk first-relapse B-cell acute lymphoblastic leukemia: a randomized clinical trial. *JAMA* 2021;325:843–54.
- Singh A, Dees S, Grewal IS. Overcoming the challenges associated with CD3+ T-cell redirection in cancer. *Br J Cancer* 2021;124:1037–48.
- Borlak J, Länger F, Spanel R, Schöndorfer G, Dittrich C. Immune-mediated liver injury of the cancer therapeutic antibody catumaxomab targeting EpCAM, CD3 and Fc γ receptors. *Oncotarget* 2016;7:28059–74.
- Fucà G, Spagnoletti A, Ambrosini M, de Braud F, Di Nicola M. Immune cell engagers in solid tumors: promises and challenges of the next generation immunotherapy. *ESMO Open* 2021;6:100046.
- Ganesan R, Chennupati V, Ramachandran B, Hansen MR, Singh S, Grewal IS. Selective recruitment of $\gamma\delta$ T cells by a bispecific antibody for the treatment of acute myeloid leukemia. *Leukemia* 2021;35:2274–84.
- Autio KA, Boni V, Humphrey RW, Naing A. Probody therapeutics: an emerging class of therapies designed to enhance on-target effects with reduced off-tumor toxicity for use in immuno-oncology. *Clin Cancer Res* 2020;26:984–9.

13. Desnoyers LR, Vasiljeva O, Richardson JH, Yang A, Menendez EE, Liang TW, et al. Tumor-specific activation of an EGFR-targeting probody enhances therapeutic index. *Sci Transl Med* 2013;5:207ra144.
14. Chomet M, Schreurs M, Nguyen M, Hwang B, Villanueva R, Krimm M, et al. The tumor targeting performance of anti-CD166 Probody drug conjugate CX-2009 and its parental derivatives as monitored by 89Zr-immuno-PET in xenograft bearing mice. *Theranostics* 2020;10:5815–28.
15. Giesen D, Broer LN, Lub-de Hooge MN, Popova I, Hwang B, Nguyen M, et al. Probody therapeutic design of 89Zr-CX-072 promotes accumulation in PD-L1-expressing tumors compared to normal murine lymphoid tissue. *Clin Cancer Res* 2020;26:3999–4009.
16. Johnson M, El-Khoueiry A, Hafez N, Lakhani N, Mamdani H, Rodon J, et al. Phase I, first-in-human study of the probody therapeutic CX-2029 in adults with advanced solid tumor malignancies. *Clin Cancer Res* 2021;27:4521–30.
17. Vasiljeva O, Hostetter DR, Moore SJ, Winter MB. The multifaceted roles of tumor-associated proteases and harnessing their activity for prodrug activation. *Biol Chem* 2019 [Online ahead of print].
18. Van Emburgh BO, Arena S, Siravegna G, Lazzari L, Crisafulli G, Corti G, et al. Acquired RAS or EGFR mutations and duration of response to EGFR blockade in colorectal cancer. *Nat Commun* 2016;7:13665.
19. Cai WQ, Zeng LS, Wang LF, Wang YY, Cheng JT, Zhang Y, et al. The latest battles between EGFR monoclonal antibodies and resistant tumor cells. *Front Oncol* 2020;10:1249.
20. Kriegs M, Clauditz TS, Hoffer K, Bartels J, Buhs S, Gerull H, et al. Analyzing expression and phosphorylation of the EGF receptor in HNSCC. *Sci Rep* 2019;9:13564.
21. Lejeune M, Köse MC, Duray E, Einsele H, Beguin Y, Caers J. Bispecific T-cell-recruiting antibodies in B-cell malignancies. *Front Immunol* 2020;11:762.
22. Lutterbuese R, Raum T, Kischel R, Hoffmann P, Mangold S, Rattel B, et al. T cell-engaging BiTE antibodies specific for EGFR potently eliminate KRAS- and BRAF-mutated colorectal cancer cells. *Proc Natl Acad Sci U S A* 2010;107:12605–10.
23. Ross SL, Sherman M, McElroy PL, Lofgren JA, Moody G, Baeuerle PA, et al. Bispecific T cell engager (BiTE[®]) antibody constructs can mediate bystander tumor cell killing. *PLoS One* 2017;12:e0183390.
24. Mosier DE, Gulizia RJ, Baird SM, Wilson DB. Transfer of a functional human immune system to mice with severe combined immunodeficiency. *Nature* 1988;335:256–9.
25. Kirberg J, Berns A, von Boehmer H. Peripheral T cell survival requires continual ligation of the T cell receptor to major histocompatibility complex-encoded molecules. *J Exp Med* 1997;186:1269–75.
26. van Rijn RS, Simonetti ER, Hagenbeek A, Hogenes MC, de Weger RA, Canninga-van Dijk MR, et al. A new xenograft model for graft-versus-host disease by intravenous transfer of human peripheral blood mononuclear cells in RAG2-/-gammac-/- double-mutant mice. *Blood* 2003;102:2522–31.
27. Wang X, Mathieu M, Brezski RJ. IgG Fc engineering to modulate antibody effector functions. *Protein Cell* 2018;9:63–73.
28. Napolitano S, Martini G, Rinaldi B, Martinelli E, Donnicuo M, Berrino L, et al. Primary and acquired resistance of colorectal cancer to anti-EGFR monoclonal antibody can be overcome by combined treatment of regorafenib with cetuximab. *Clin Cancer Res* 2015;21:2975–83.
29. Cibrián D, Sánchez-Madrid F. CD69: from activation marker to metabolic gatekeeper. *Eur J Immunol* 2017;47:946–53.
30. Simms PE, Ellis TM. Utility of flow cytometric detection of CD69 expression as a rapid method for determining poly- and oligoclonal lymphocyte activation. *Clin Diagn Lab Immunol* 1996;3:301–4.
31. Kamakura D, Asano R, Kawai H, Yasunaga M. Mechanism of action of a T cell-dependent bispecific antibody as a breakthrough immunotherapy against refractory colorectal cancer with an oncogenic mutation. *Cancer Immunol Immunother* 2021;70:177–88.
32. Kist de Ruijter L, Hooiveld-Noeken JS, Giesen D, Lub-de Hooge MN, Kok IC, Brouwers AH, et al. First-in-human study of the biodistribution and pharmacokinetics of 89Zr-CX-072, a novel immunopet tracer based on an anti-PD-L1 Probody. *Clin Cancer Res* 2021;27:5325–33.
33. Tang T, Huang X, Zhang G, Hong Z, Bai X, Liang T. Advantages of targeting the tumor immune microenvironment over blocking immune checkpoint in cancer immunotherapy. *Signal Transduct Target Ther* 2021;6:72.
34. Labani-Motlagh A, Ashja-Mahdavi M, Loskog A. The tumor microenvironment: a milieu hindering and obstructing antitumor immune responses. *Front Immunol* 2020;11:940.
35. Ahmed D, Eide PW, Eilertsen IA, Danielsen SA, Eknæs M, Hektoen M, et al. Epigenetic and genetic features of 24 colon cancer cell lines. *Oncogenesis* 2013;2:e71.
36. Crawford A, Haber L, Kelly MP, Vazzana K, Canova L, Ram P, et al. A Mucin 16 bispecific T cell-engaging antibody for the treatment of ovarian cancer. *Sci Transl Med* 2019;11:eaa7534.
37. Sam J, Colombetti S, Fauti T, Roller A, Biehl M, Fahrni L, et al. Combination of T-cell bispecific antibodies with PD-L1 checkpoint inhibition elicits superior anti-tumor activity. *Front Oncol* 2020;10:575737.
38. Study evaluating safety, tolerability and PK of AMG 757 in adults with small cell lung cancer. *ClinicalTrials.gov* identifier: NCT03319940 updated February 21, 2022. Accessed March 25, 2022. Available from: <https://clinicaltrials.gov/ct2/show/NCT03319940>.
39. Safety, tolerability, pharmacokinetics, and efficacy of acapatamab in subjects with mCRPC. *ClinicalTrials.gov* identifier: NCT03792841 Updated March 4, 2022. Accessed March 25, 2022. Available from: <https://clinicaltrials.gov/ct2/show/NCT03792841>.
40. A study of the safety, pharmacokinetics, and therapeutic activity of RO6958688 in combination with atezolizumab in participants with locally advanced and/or metastatic carcinoembryonic antigen (CEA)-positive solid tumors. *ClinicalTrials.gov* identifier: NCT02650713 Updated February 12, 2020. Accessed March 25, 2022. Available from: <https://clinicaltrials.gov/ct2/show/NCT02650713>.
41. Safety and efficacy of XmAb18087 ± pembrolizumab in advanced merkel cell carcinoma or extensive-stage small cell lung cancer. *ClinicalTrials.gov* identifier: NCT04590781 Updated January 26, 2022. Accessed March 25, 2022. Available from: <https://clinicaltrials.gov/ct2/show/NCT04590781>.
42. REGN4336 (a PSMAXCD3 bispecific antibody) administered alone or in combination with cemiplimab in adult male patients with metastatic castration-resistant prostate cancer. *ClinicalTrials.gov* identifier: NCT05125016 Updated March 10, 2022. Accessed March 25, 2022. Available from: <https://clinicaltrials.gov/ct2/show/NCT05125016>.
43. Study of REGN4018 administered alone or in combination with cemiplimab in adult patients with recurrent ovarian cancer. *ClinicalTrials.gov* identifier: NCT03564340. Updated February 23, 2022. Accessed March 25, 2022. Available from: <https://clinicaltrials.gov/ct2/show/NCT03564340>.
44. Study of REGN5668 administered in combination with cemiplimab or REGN4018 in adult women with recurrent ovarian cancer. *ClinicalTrials.gov* identifier: NCT04590326 Updated March 21, 2022. Accessed March 25, 2022. Available from: <https://clinicaltrials.gov/ct2/show/NCT04590326>.
45. Erbitux (cetuximab). Prescribing information. ImClone LLC a wholly-owned subsidiary of Eli Lilly and Company; 2021. Available from: https://www.access.data.fda.gov/drugsatfda_docs/label/2021/125084s277s280lbl.pdf.
46. Panchal A, Seto P, Wall R, Hillier BJ, Zhu Y, Krakow J, et al. COBRA[™]: a highly potent conditionally active T cell engager engineered for the treatment of solid tumors. *MAbs* 2020;12:1792130.
47. Stroh M, Green M, Millard BL, Apgar JF, Burke JM, Garner W, et al. Model-informed drug development of the masked anti-PD-L1 antibody CX-072. *Clin Pharmacol Ther* 2021;109:383–93.
48. Etxeberria I, Bolaños E, Teixeira A, Garasa S, Yanguas A, Azpilikueta A, et al. Antitumor efficacy and reduced toxicity using an anti-CD137 probody therapeutic. *Proc Natl Acad Sci U S A* 2021;118:e2025930118.
49. Naing A, Thistlethwaite F, De Vries EGE, Eskens FALM, Uboha N, Ott PA, et al. CX-072 (pacmilimab), a Probody[®] PD-L1 inhibitor, in advanced or recurrent solid tumors (PROCLAIM-CX-072): an open-label dose-finding and first-in-human study. *J Immunother Cancer* 2021;9:e002447.
50. Boni V, Fidler MJ, Arkenau HT, Spira A, Meric-Bernstam F, Uboha N, et al. Praluzatamab ravtansine, a CD166-targeting antibody-drug conjugate, in patients with advanced solid tumors: an open-label phase I/II trial. *Clin Cancer Res* 2022;28:2020–9.
51. Crawford A, Chiu D. Targeting solid tumors using CD3 bispecific antibodies. *Mol Cancer Ther* 2021;20:1350–8.
52. Middelburg J, Kemper K, Engelberts P, Labrijn AF, Schuurman J, van Hall T. Overcoming challenges for CD3-bispecific antibody therapy in solid tumors. *Cancers* 2021;13:287.